VIII International Conference on Fracture Mechanics of Concrete and Concrete Structures
FraMCoS-8
J.G.M. Van Mier, G. Ruiz, C. Andrade, R.C. Yu and X.X. Zhang (Eds)

CONTROL OF CRACKING IN R.C. STRUCTURES: NUMERICAL SIMULATION OF A SQUAT SHEAR WALL

C. DAMONI[*], B. BELLETTI[†] AND G. LILLIU[#]

[*] University of Parma
Parco Area delle Scienze 181/A,43124 Parma, Italy
e-mail: cecilia.damoni@nemo.unipr.it

[†] University of Parma
Parco Area delle Scienze 181/A, 43124 Parma, Italy
e-mail: beatrice.belletti@unipr.it

[#] TNO DIANA BV
Delftechpark 19ª, 2628XJ Delft, The Netherland
e-mail: G.Lilliu@tnodiana.com

Key words: squat shear wall, shear resistance, nonlinear finite element analyses, safety levels

Abstract: In this paper the behavior of a squat shear wall subjected to monotonic shear loading is investigated. The study fits into the experimental program driven by CEOS.fr on modeling of the behavior of the tested mocks-ups (monotonic and cycling loading-under prevented or free shrinkage). The shear wall has been analyzed with nonlinear finite element analyses carried out with the finite element code DIANA and numerical results have been compared with the experimental results presented during the Concrack2 Benchmark Workshop that has been held in Paris in 2011. The design shear resistance of the shear wall has been also evaluated with analytical and numerical procedures according to the new Model Code 2010 prescriptions. The analytical calculations, which have been carried out with a strut and tie model, have been compared with numerical results from nonlinear finite element analyses.

1 INTRODUCTION

In this paper the behavior of a squat shear wall subjected to monotonic shear loading is investigated. The study fits into the experimental program driven by [1] on modeling the behavior of the tested mocks-ups (monotonic and cycling loading-under prevented or free shrinkage). The shear wall analyzed was tested in laboratory by [1] and the experimental results have been presented during the last Concrack2 Benchmark Workshop [2].

The shear wall has been analyzed by means of nonlinear finite element (NLFE) analyses that have been carried out with the finite element code DIANA [3] and the obtained numerical results have been compared with the available experimental results.

It is well known that NLFE analyses allow for more realist modelling of material and structural behaviour and, in this manner, can account for additional bearing capacity of the structure. Nevertheless, the results obtained from NLFE analyses strongly depend on the assumptions made in the model, especially when crack models are used. It is known that, especially for shear-critical specimens, aggregate interlock, tension stiffening, multi-axial stress states and Poisson's effects play all an important role in the structural response. For this reason, if the sensitive parameters are

not well calibrated during the modelling phase, a large scatter can be expected in the results. For this reason, and in order to properly calibrate parameters of the adopted crack model, a parametric study has been carried out on the wall. The numerical model of the squat wall has been developed following some guidance for nonlinear finite element analyses proposed and further investigated in [4] and [5].

After calibration of the model, the numerical analyses have been able to predict well the general behavior of the squat wall both in terms of shear resistance-maximum displacement trend and in terms of failure mode.

Furthermore the design shear resistance of the squat wall has been evaluated following the prescriptions of the new Model Code 2010 [6]. The Model Code 2010 [6] proposes different calculation methods for the evaluation of the design shear resistance of slender and squat elements.

For slender elements (e.g. reinforced and prestressed concrete beams and slabs) the design shear resistance can be evaluated through analytical and numerical calculation methods that belong to different Levels of approximation: by increasing the level of approximation the complexity and the accuracy of the results obtained increases. Level of approximation I, II and III refer to analytical calculation methods (hand calculations) while the highest level of approximation, Level of approximation IV, refers to numerical methods, performed with NLFE analyses. Within Level IV the results obtained from NLFE analyses are properly reduced in order to obtain the same safety level of analytical calculations. To this aim the new Model Code 2010 [6] proposes three alternative methods, denoted as “safety format methods” that properly reduce the shear resistance obtained from nonlinear finite element analyses, in order to obtain the same safety level obtained from analytical calculations.

The safety format methods are so denoted: Partial Factor method (PF), Global Resistance Factor method (GRF) and Estimation of Coefficient of Variation of resistance method (ECOV).

For squat elements the Model Code 2010 [6] recommends that the design shear resistance is evaluated with a strut and tie model.

In this paper the design shear resistance of the squat wall has been evaluated analytically with a strut and tie model. Furthermore the prescriptions of Level IV have been also applied to the wall. The results obtained from NLFE analyses have therefore been reduced according to the safety format methods prescriptions and compared to the analytical results.

2 EXPERIMENTAL SET-UP

The squat shear wall was clamped at the top and at the bottom in two highly reinforced beams and the left and right extremities were seamed with rebars. The wall was placed in a rigid metallic frame and subjected to monotonic loading-unloading through two jacks placed at the top of the wall, Figure 1.

(a)

(b)

Figure 1: (a) Experimental set-up, (b) Reinforcement layout and boundary conditions.

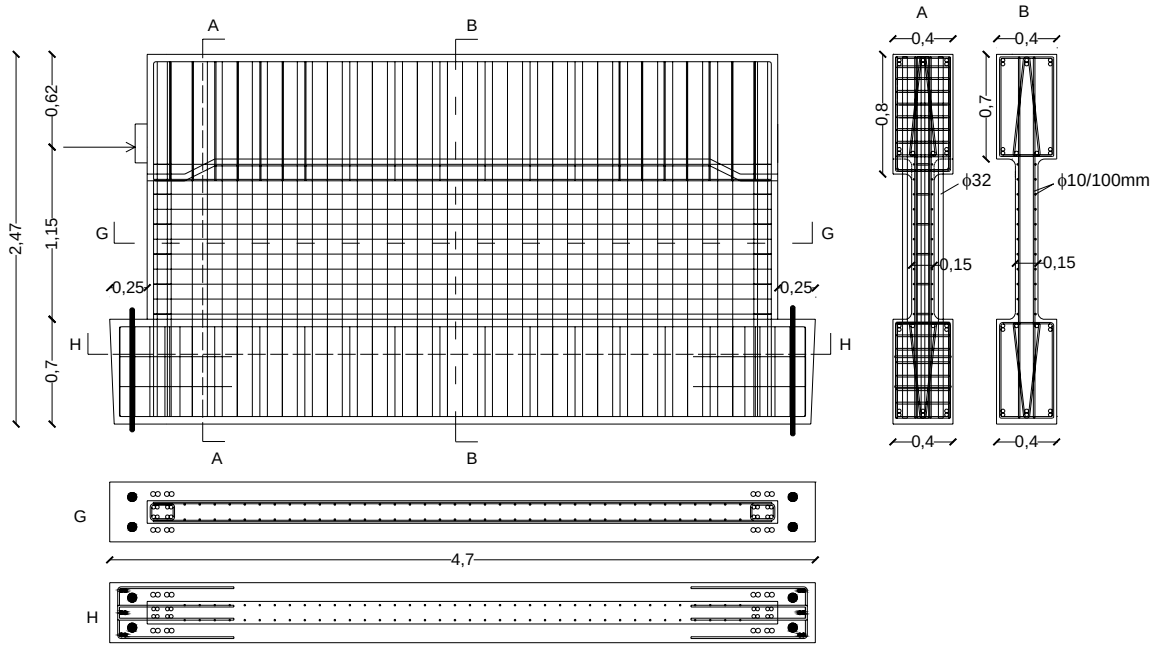

Figure 2: Reinforcement layout (dimension in m).

Experimental sensors were placed on the two faces of the wall in order to measure the crack width and the strain in the rebars. In Table 1 the mean mechanical properties of concrete and steel, measured during the experimental test, are reported.

Table 1: Mean mechanical properties of materials.

Concrete		**Steel**	
f_c [N/mm^2]	-42.5	f_y [N/mm^2]	554
f_t [N/mm^2]	3.3	E_s [N/mm^2]	189274
E_c [N/mm^2]	22060	f_u [N/mm^2]	634
ν	0.19		

In Figure 2 the reinforcement layout of the wall is plotted. The total length of the wall is 4.7 m, the total height is 2.47m and the main reinforcement grid, placed in the web panel, is made of ϕ10/100 mm. The web panel is 4.2m x 1.15m. Further geometrical details are available in [2].

According to the experimental test the wall failed in shear due to crushing of concrete under the loading plate and the reinforcement remained elastic up to failure. The maximum load measured in the test was $P_{u,exp}$=4710 KN.

The experimental crack pattern is shown in Figure 3 for some load levels.

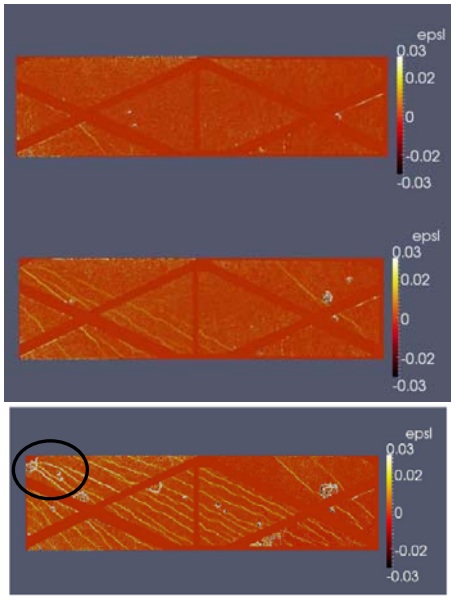

Figure 3: Experimental crack pattern.

3 FINITE ELEMENT MODEL

Nonlinear finite element analyses have been carried out on the wall with the code DIANA [3] using a 2D model.

Eight- nodes quadrilateral isoparametric plane stress elements based on quadratic interpolation and (3x3) Gauss integration scheme have been adopted for modeling the wall and the loading plate. Embedded reinforcement elements, with the hypothesis of perfect bond, have been used to model reinforcement. The two lateral ϕ32 bars, located at the extremities of the wall, outside the wall web, have been modeled with truss elements. Six-nodes interface elements have been inserted between the loading plate and the concrete wall. Average element dimensions in the mesh of the wall are 100mm x 100 mm. Displacements in *x* direction have been set all equal for the nodes along the line of loading.

The analyses have been carried out in load control using a regular Newton-Raphson convergence criterion based on energy and force control. The mesh adopted and the boundary conditions used in the analyses are shown in Figure 4.

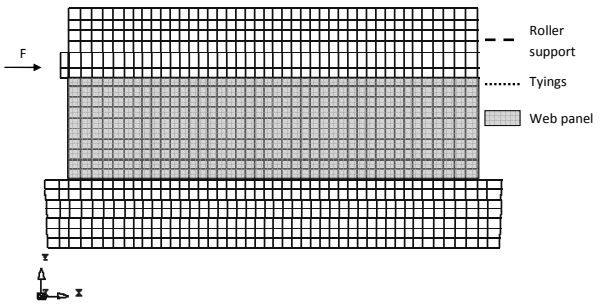

Figure 4: Mesh and boundary conditions adopted in the finite element model.

3.1 Constitutive model and crack model

Only the web panel (grayed in Figure 4) has been modeled with a nonlinear behavior, while the flanges of the wall have been modeled as elastic.

For the web panel a parabolic law in compression and an exponential law in tension have been adopted. The compressive fracture energy and the tensile fracture energy values have been determined respectively according to [7] and [6], Figure 5(a). For the reinforcement an elastic-plastic behaviour with hardening has been used, Figure 5(b).

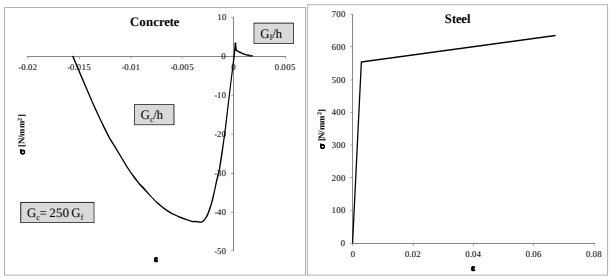

(a) (b)

Figure 5: Constitutive model of (a) concrete and (b) steel.

A total strain rotating crack model has been adopted in the analyses [8]. In the parametric study, the results obtained with the rotating crack model have been compared with those one obtained with a total strain fixed crack model.

The rotating crack model used [8] is based on the concept of co-axiality between stress and strain. The strain referred to *ns* coordinate system ${}^{t+\Delta t}_{i+1}\varepsilon_{ns}$ is substituted by the equivalent uni-axial strain ${}^{t+\Delta t}_{i+1}\tilde{\varepsilon}_{ns}$ to take into account the lateral expansion due to the Poisson's effect, eq.(1):

$$ {}^{t+\Delta t}_{i+1}\tilde{\varepsilon}_{ns} = \begin{bmatrix} \frac{1-\nu}{(1+\nu)(1-2\nu)} & \frac{\nu}{(1+\nu)(1-2\nu)} \\ \frac{\nu}{(1+\nu)(1-2\nu)} & \frac{1-\nu}{(1+\nu)(1-2\nu)} \end{bmatrix} {}^{t+\Delta t}_{i+1}\varepsilon_{ns} \qquad (1) $$

According to the model implemented in DIANA [3] the Poisson's coefficient linearly decreases from its initial value up to zero as the residual tensile stress becomes zero.

Contrary to the rotating crack model, the fixed crack model provides that the orthotropic material coordinate system *ns* remains fixed after the appearance of the primary cracking so that shear stresses develop along the crack face. The shear stresses depend on the shear stiffness reduced by a coefficient called "shear retention factor β". Eq.(2) gives the stiffness matrix *D* that is used in the fixed crack model:

$$ D = \begin{bmatrix} \frac{E_n}{1-\nu_{ns}\nu_{sn}} & \frac{\nu_{sn}E_n}{1-\nu_{ns}\nu_{sn}} & 0 \\ \frac{\nu_{ns}E_s}{1-\nu_{ns}\nu_{sn}} & \frac{E_s}{1-\nu_{ns}\nu_{sn}} & 0 \\ 0 & 0 & G_{ns} \end{bmatrix} \qquad (2) $$

E_n ,E_s represent the elastic moduli in the cracked phase, ν_{ns} e ν_{sn} are the Poisson's coefficients, G_{ns} is the reduced shear stiffness, $G_{ns} = \beta G$ where β is the shear retention factor. In the model that is used for these analyses, β decreases linearly from 1 (in the elastic phase) up to zero as the crack width is nearly equal to half of the aggregate size.
Besides the Poisson's effect, also effects of biaxial stress states on the compressive strength of concrete are taken into account in the model. Reduction of the compressive strength due to lateral cracking follows the Model B of Vecchio et. al. [9], Figure 6. According to this model only the compressive strength and not the peak strain is reduced, leading to a reduction of the Young's modulus already in the elastic phase.

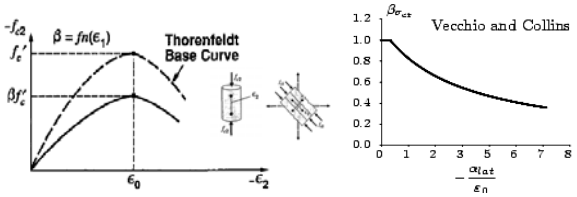

Figure 6: Multi-axial stress state: reduction of the compressive strenght due to lateral cracking [9].

A more refined structural assessment can in general be obtained if some important parameters of the crack model like aggregate interlock effect, tension stiffening, multi-axial stress-state etc. are taken into account in the material model [10], [11], [12], [13], [14].

4 EVALUATION OF THE DESIGN SHEAR RESISTANCE ACCORDING TO MC2010

As mentioned in section 1 the design shear resistance of the wall has been evaluated analytically according to a strut and tie model and numerically applying the prescriptions of Level IV approximation.

Within Level IV the same safety level obtained with analytical procedures can be obtained with three safety format methods: the Global Resistance Factor method (GRF), the Partial Factor method (PF) and the Estimation of Coefficient of Variation of resistance method (ECOV).

4.1 Analytical procedure: strut and tie model

Structures can be subdivided into *B*-regions, where the assumption of a plane section may be used and *D*-regions, typically located at supports or at places of concentrated loads, where a non-linear strain distribution exists.
For the analyses the design shear resistance R_d has been evaluated according to the strut and tie model proposed in the Model Code 2010 [6] and according to prescriptions available in literature. A schematization of the adopted strut and tie model is reported in Figure 7.

$$R_d = \sigma_{Rd,max} \cdot A_{str} \cdot \cos\theta \tag{3}$$

where θ is the strut inclination angle, $\sigma_{Rd,max}$ is the maximum stress at the edge of the node, (4):

$$\sigma_{Rd,max} = \frac{k_c \cdot f_{ck}}{\gamma_c} \tag{4}$$

For compression-tension nodes with anchored ties provided in one or two directions k_c is determined as:

$$k_c = 0.75 \cdot \eta_{fc}\,;\eta_{fc} = \left(\frac{30}{f_{ck}}\right)^{1/3} \le 1 \tag{5}$$

A_{str} is the area of the concrete strut, eq. (6):

$$A_{str} = t_w \cdot a_s \tag{6}$$

where t_w is the web thichness and a_s is the width of the concrete strut. According to [15] and adopted in [16] the width of the concrete strut can be determined as:

$$a_s = \left(0.25 + 0.85\frac{N}{A_w f_c'}\right) \cdot l_w \tag{7}$$

where l_w is the wall lenght.
The corresponding values of all parameters in play are in Table 2.

Table 2: Mechanical parameters used in the strut and tie calculation.

θ [°]	k_c	γ_c	l_w [m]	N [KN]
12	0.716	1.5	4.2	0

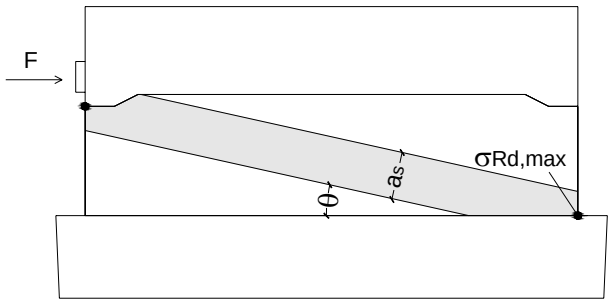

Figure 7: (a) Schematizaton of the squat wall according to the strut and tie model used.

4.2 Numerical procedures: Level of Approximation IV

According to the GRF method, the input values of the mechanical material properties are the mean values. The global resistance of the structure R_d, obtained from NLFE analyses, is considered as a random variable so that the effects of various uncertainties are integrated in a global design resistance expressed by a global safety coefficient (equal to 1.27), eq. (8).

$$R_d = \frac{R(f_m,...)}{\gamma_R \gamma_{Rd}} = \frac{R(f_m,...)}{1.2 \cdot 1.06} = \frac{R(f_m,...)}{1.27} \quad (8)$$

According to the PF method, the design mechanical material properties are according to the fib Model Code prescriptions. Therefore the shear resistance of the structure $R_{d,}$ from NLFE analysis is already the design shear resistance (eq. (9)).

$$R_d = R(f_d,...) \quad (9)$$

According to the ECOV method, two analyses must be carried out with mean and characteristic values of mechanical material properties, respectively. This method is based on the assumption of a lognormal distribution of the resistance, thus the coefficient of variation of resistance follows from the two calculated resistances (eq. (10), (11)).

$$R_m = R(f_m,...), R_k = R(f_k,...); \quad R_d = \frac{R_m}{\gamma_R \gamma_{Rd}} \quad (10)$$

$$\gamma_R = exp(\alpha_R \beta V_R) = exp\left(0.8 \cdot 3.8 \cdot \left[\frac{1}{1.65} ln(R_{meas}/R_k)\right]\right) \quad (11)$$

Starting from the mean values of the mechanical material properties,obtained from experimental measurments, characteristic and design mechanical properties have been derived as reported in Table 3 ("m" refers to mean mechanical properties).

Table 3: Characteristic and design mechanical material properties according to Model Code 2010.

Characteristic	Design
$f_{ck} = f_{cm} - 8$	$f_{cd} = f_{ck}/1.5$
$f_{tk} = 0.7 f_{tm}$	$f_{td} = f_{tk}/1.5$
$E_{ck} = 21500\left(\frac{f_{ck}}{10}\right)^{1/3}$	$E_{cd} = 21500\left(\frac{f_{cd}}{10}\right)^{1/3}$
$G_{fk} = 73 f_{ck}^{0.18}$	$G_{fd} = 73 f_{cd}^{0.18}$
$f_{yk} = f_{ym}/1.1$	$f_{yd} = f_{yk}/1.15$
$f_{uk} = f_{um}/1.1$	$f_{ud} = f_{uk}/1.15$

5 RESULTS

As mentioned in the previous sections a parametric study has been carried out on the shear wall in order to properly calibrate some important parameters of the crack model. In Figure 8 the load-deflection curves obtained from the parametric study is reported. All the analyses within the parametric study have been carried out using mean values of the mechanical materials properties. For sake of simplicity a monotonic loading has been applied to the wall. In the adopted crack model the unloading is modeled as secant unloading with zero residual strain. The displacement reported in Figure 8 is the relative horizontal displacement measured between the top of the lower beam and the bottom of the upper beam. The legend reported in Figure 8 has the following meaning:

- **Analysis A**:
  -fixed crack model;
  -variable Poisson's coefficient. The Poisson's coefficient linearly decreases from 0.19 in the elastic phase up to 0.0 as the residual tensile stress becomes zero;
  -variable shear retention factor;
  -maximum reduction of the compressive strength due to lateral cracking is 40% ($f_{c,red}/f_c$=0.6);

-tensile fracture energy G_f according to Model Code 2010 ($G_{f,MC2010} = 73 f_c^{0.18}$).

- **Analysis B**:
  -rotating crack model;
  -variable Poisson's coefficient The Poisson's coefficient linearly decreases from 0.19 in the elastic phase up to 0.0 as the residual tensile stress becomes zero;
  -maximum reduction of the compressive strength due to lateral cracking is 40% ($f_{c,red}/f_c=0.6$);
  -tensile fracture energy G_f according to Model Code 2010 ($G_{f,MC2010} = 73 f_c^{0.18}$).
- **Analysis C**:
  -rotating crack model;
  -variable Poisson's coefficient The Poisson's coefficient linearly decreases from 0.19 in the elastic phase up to 0.0 as the residual tensile stress becomes zero;
  -maximum reduction of the compressive strength due to lateral cracking is 40% ($f_{c,red}/f_c=0.6$);
  -tensile fracture energy is modified to take into account the tension stiffening effect.

Since the assumption of perfect bond is made, tension stiffening is taken into account by increasing the value of the tensile fracture energy G_f ,in order to obtain for concrete the same ultimate strain as the yield strain of the reinforcement bars. This has been achieved in Analysis C considering $G_f = 1.75 G_{f,MC2010}$.

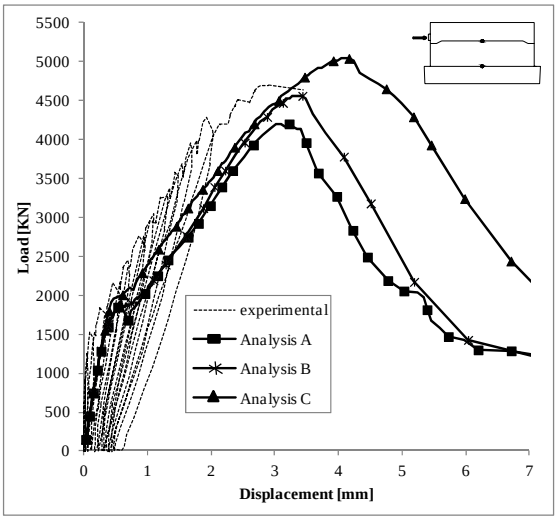

Figure 8: Parametric study: load-displacement curves.

From Figure 8 it can be noted that the load-deflection curve that better fits the experimental curve both in terms of maximum load reached and in terms of maximum displacement. is obtained with Analysis B For this reason Analysis B has been chosen as reference analysis for the application of the safety format methods.

In Figure 9 crack pattern obtained from Analysis B at different levels of load is plotted in terms of tensile cracking strain. Figure 10 shows the compressive strains.

In Figure 11 the load-crack width diagram of crack number 9 predicted in Analysis B is compared to the experimental diagram.

The crack width has been obtained multiplying the tensile strain obtained from the numerical analysis by the crackbandwidth $h = \sqrt{A_{elem}}$.

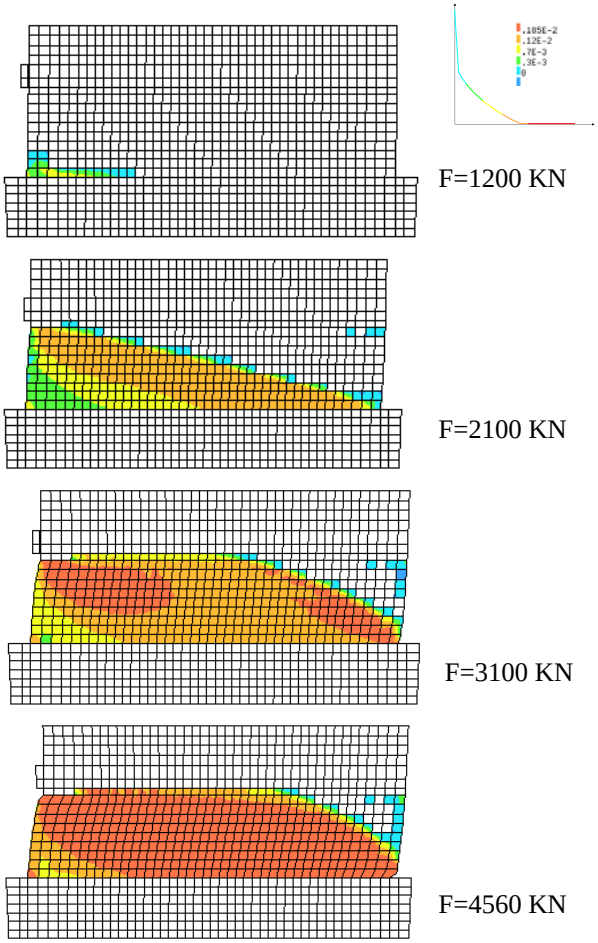

Figure 9: Tensile cracking strain of concrete for some significant load steps of Analysis B.

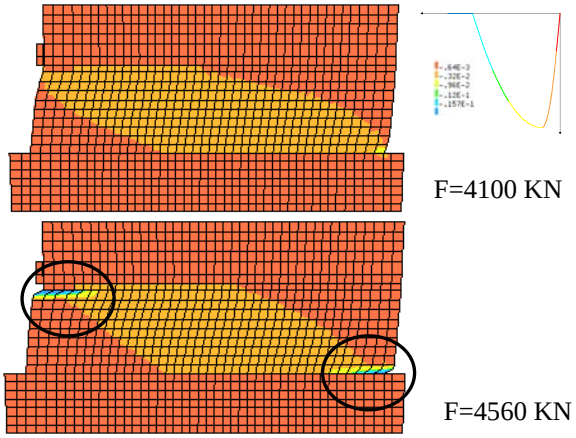

Figure 10: Compressive strain of concrete for some significant load steps of Analysis B.

Comparing Figure 9, Figure 10 and Figure 11 with Figure 3 it can be noted that the general behavior of the wall has been well predicted by numerical simulations also in terms of failure mode. The wall in fact failed in shear due to crushing of concrete under the loading plate and at the bottom right corner while the reinforcement remained elastic untill failure.

The finite element model used in Analysis B has been chosen as reference to carry out the analyses applying the safety format methods [6]. In Table 4 the design shear resistance values obtained analytically, with the strut and tie model and numerically, with the safety format methods, are compared to the experimental shear resistance. The shear resistance obtained from Analysis B, which has been carried out using mean values of the mechanical material properties without applying any safety coefficients, is also reported in Table 4.

Table 4: Design shear resistance values.

		P_u [KN]
	Experimental	4710
Mean values	Analysis B (no safety format)	4560
Design shear resistance	Analytical (strut and tie)	2536
	Level IV- GRF	3585
	Level IV- PF	2994
	Level IV- ECOV	3364

In Figure 12 the design shear resistance values P_u obtained with analytical and numerical procedures by applying the safety format methods are reported in histograms as a percentage of the experimental shear resistance $P_{u,exp}$. Furthermore the ratio $P_u/P_{u,exp}$ is also reported for Analysis B. Grey histograms refer to the design shear resistance values obtained analytically and numerically while the white histogram refers to the shear resistance obtained from Analysis B. It can be noted that NLFE analysis carried out with mean values (Analysis B) provides a good prediction of the wall shear capacity.

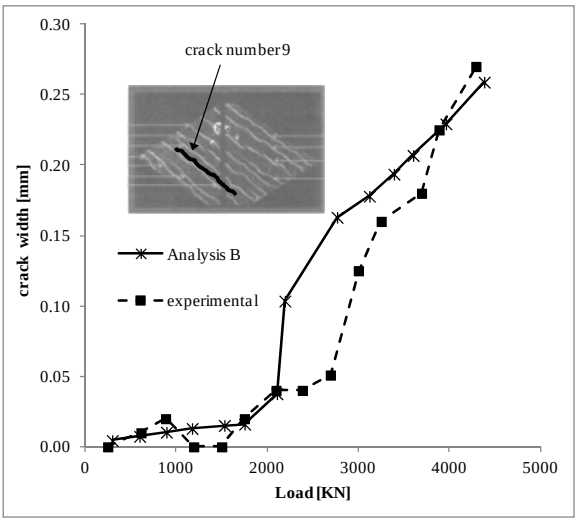

Figure 11: Load-crack width curve.

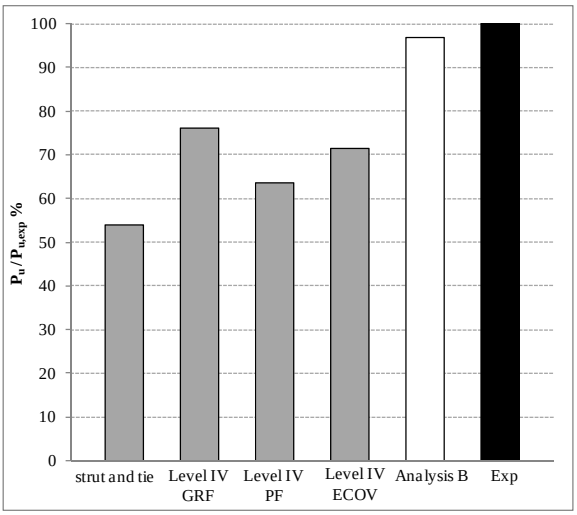

Figure 12: Design shear resistance values P_u obtained analytically (strut and tie) and numerically (Level IV), expressed as a percentage of the experimental shear resistance $P_{u,exp}$.

Figure 12 shows that the results obtained applying the safety format methods well match with the philosophy of the Levels of

approximation: by increasing the Level of approximation the accuracy of the results increases and the maximum resistance of the structure increases. The design shear resistance values obtained from NLFE analyses (Level IV) are indeed higher than the design shear resistance value obtained with analytical calculation (strut and tie model).

6 CONCLUSIONS

In this paper the behavior of a squat shear wall subjected to monotonic loading has been investigated by means of analytical procedures and nonlinear finite element analyses. The results obtained have been compared with the experimental results available. The study fits into the experimental program driven by CEOS.fr on modeling the behavior of the tested mocks-ups. The main results of the research are listed below.

- The shear wall has been analyzed with a 2D finite element model, using the commercial finite element program DIANA
- A parametric study has been carried out on the shear wall in order to focus on the main sensitive parameters that influence the results of nonlinear finite element analyses Special attention has been given to the effects on the results of the material properties adopted in the crack model (tensile strength and fracture energy). The numerical model has been calibrated referring to the available experimental results.
- After having calibrated the numerical model, the general behavior of the shear wall has been well predicted by NLFE analyses both in terms of load-displacement diagram and in terms of failure mode.. The scatter in the shear resistance value is about 3%. The numerical simulation has also predicted failure of the wall in shear due to crushing of concrete under the loading plate and in the bottom right corner without yielding of reinforcement.
- The design shear resistance of the wall has been also determined following the Model Code 2010 prescriptions. The Model Code 2010 proposes different calculation methods for the evaluation of the design shear resistance of slender and squat elements. For squat elements the design shear resistance can be determined analytically with a strut and tie model.
  On the contrary the design shear resistance for slender elements can be determined according to four Levels of approximations. Level of approximation I, II and III refer to analytical procedures while Level IV refers to the results obtained from NLFE analyses, properly reduced in order to obtain the same safety level of analytical procedures. To this aim the Model Code 2010 proposes three different safety format methods (GRF, PF, ECOV).
- In this paper the design shear resistance of the wall has been evaluated analytically with a strut and tie model, since the wall is a squat shear wall. Furthermore the prescriptions of Level IV have been also applied to the wall. The results obtained from NLFE analyses have therefore been reduced according to the safety format methods prescriptions and compared to the analytical results.
- The results obtained well match with the philosophy of the Model Code 2010: by increasing the Level of approximation the design shear resistance value increases.
  The design shear resistance values obtained applying the safety format methods (Level IV) are in fact as higher as 40% than the design shear resistance obtained with analytical calculations (strut and tie model).
- The structural assessment carried out with the Levels of approximation can be of big utility for intervention plans on existing structures (e.g. maintenance, repair, demolition etc.) with regard to sustainability criteria.

REFERENCES

[1] French national research programme CEOS.fr: Behaviour and assessment of special construction works concerning cracking and shrinkage.

[2] Rospars, C., Delapalce A., 2010. Synthesis results related to Shear Wall. *2nd*

Workshop on Control of Cracking in R.C. Structures, 20-22 June 2010, Paris, France.

[3] Manie, J., 2009. DIANA user's manual. TNO DIANA BV.

[4] Rots, J., Belletti, B., Damoni, C., Hendriks, M.A.N., 2010. Development of Dutch guidelines for nonlinear finite element analyses of shear critical bridge and viaduct beams. *fib Bulletin 57: Shear and punching shear in RC and FRC elements*, pp. 139-154.

[5] Belletti, B., Damoni, C., Hendriks, M.A.N., 2011. Development of guidelines for nonlinear finite element analyses of existing reinforced and pre-stressed beams. *European Journal of Environmental and Civil Engineering*, **15** (9):1361-1384.

[6] CEB-FIP bulletin d'information 65&66 - Model Code MC2010 - Final Draft, International Federation for Structural Concrete (fib), Lausanne, Switzerland. 2012.

[7] Nakamura, H., Higai, T., 2001. Compressive Fracture Energy and Fracture Zone Length of Concrete. *Modeling of inelastic behaviour of RC structures under seismic loads*, P.Benson Shing Tada-aki Tanabe (eds), pp. 471-487.

[8] Feenstra, P.H., Rots, J.G., Arnesen, A., Teigen, J.G., Hϕiseth, K.V., 1998. A 3D constitutive model for concrete based on a co-rotational concept. *Computational Modelling of Structures*, de Borst, Bicanic, Mang & Meschke (eds), Balkema.

[9] Vecchio, F.J., Collins, M.P., 1986. The modified compression-field theory for reinforced concrete elements subjected to shear. *ACI Struct. Journal*, **83**(2):219-231.

[10] Walraven, J.C., 1981. Fundamental analysis of aggregate interlock. *J. Struct. Eng.*, **107**(11):2245-2270.

[11] Belletti, B., Cerioni, R., Iori, I., 2001. A Physical Approach for Reinforced Concrete (PARC) membrane elements. *J. Struct. Eng.*, **127**(12):1412-1426.

[12] Hsu, T.T.C., Mo, Y.L., 2010. Unified theory of concrete structures. *John Wiley and Sons, Ltd, Publication*.

[13] Walraven, J.c., Belletti, B., Esposito, R., 2012. Shear capacity of normal, lightweight & high-strength concrete beams according to MC2010. Part I., *J. Struct. Eng.*, in press.

[14] Belletti, B., Esposito, R., Walraven, J.C.,2012. Shear capacity of normal, lightweight & high-strength concrete beams according to MC2010. Part II. , *J. Struct. Eng.*, in press.

[15] Paulay, T., Priestley, M. J. N., 1992. Seismic design of reinforced concrete and masonry buildings. *Wiley, New York*.

[16] Shyh-Jiann Hwang, S.J., Wen-Hung Fang, W.H., Lee, H.J, Yu, H.W., 2001. Analytical Model for predicting shear strength of squat walls. *Journal of Structural Engineering*, **127**(1): 43-50.